Investigation the Solubility of Anthraquinone Violet 3RN in Supercritical Carbon Dioxide

M. Amani
Department of Chemical Engineering, Robat Karim Branch, Islamic Azad University, Robat Karim, Iran.
Mitraamani58@gmail.com

Abstract
The solubility of Anthraquinone Violet 3RN (AV3RN) was measured in supercritical CO_2 (sc-CO_2) at different temperatures (308–338K) and pressures (10-34MPa). The solubility of AV3RN varied in the range of 4.7×10^{-7} to 5.5×10^{-6} mole fractions. Obtained solubility data was correlated with several density-based models. Empirical models developed by Khansary *et al*. along with Garlapati-Madras models exhibited the highest accordance with experimental data. Also, it was shown that AV3RN evaporation is an endothermic process while its solvation is an exothermic process.

Keywords: Anthraquinone Violet 3RN (AV3RN); Supercritical carbon dioxide (sc-CO_2); Empirical models; Solubility

Introduction
Anthraquinones are aromatic organic compounds from the quinone family. The term "anthraquinone" refers to one specific isomer in which the ketone groups are located on the central ring at C-9 and C-10 positions [1]. Anthraquinone Violet 3RN (AV3RN) ($C_{28}H_{20}N_2Na_2O_8S_2$) is an organometallic pigment and a synthetic anionic dye with wide range of applications among which foodstuffs, plastic and cosmetics industries and textile industry can be mentioned [2]. The textile industry is known as one the most important environment polluting industries. Its wastewater treatment is so difficult due to existence of large amounts of water, dyes and chemical additives which were consumed in conventional dyeing processes [3]. AV3RN is one of these dyes known for its high chemical/biological oxygen demand, solid suspensions and high toxicity. Degradation and elimination of AV3RN dye is difficult due to presence of the fused aromatic rings and sulfonated groups making the mentioned dye a renitent and carcinogenic substance [4].
Eliminating the process water and chemicals could dramatically improve the textile dyeing industry. It sounds to be accomplished by the advent of the innovative dyeing machines employing supercritical fluids (SCF) instead of the water [5]. Carbon dioxide is one of the favorite supercritical solvents as it is accessible, recyclable, easy to handle, inexpensive, non-toxic, nonflammable and has low critical temperature. In a supercritical dyeing process, dye solubility in supercritical carbon dioxide (sc-CO_2) plays a significant role as the dyes should be dissolved in sc-CO_2 phase and diffused into the fibers. Dye solubility and diffusion is

greatly affected by sc-CO_2 density, due to the major effect of molecular interaction between the dye and sc-CO_2 molecules. Therefore, further development and optimization of supercritical dyeing process requires the data on dyes solubility in supercritical fluids under various conditions. Moreover, these data should be accurately modeled by various thermodynamic approaches (i.e. equations of state (EOS) and empirical models).
Literature review shows that the solubility of anthraquinone Violet 3RN (AV3RN) dye, in sc-CO_2 has been never addressed. So, the present research is the first attempt to investigate the solubility of AV3RN in sc-CO_2 at various temperatures 308–338K and pressures 10-34MPa. These experimental results were correlated by different empirical models

Experimental and modelling

In a typical procedure, once passed through a filter, carbon dioxide enters a refrigerating unit and converted to liquid through temperature reduction from room temperature to ~-4 ºC. The pressure of the liquefied CO_2 is adjusted to a desired pressure by a high pressure pump. The temperature is maintained by placing the equilibrium cell in an oven. Solubility was performed in a 100 ml extraction cell at the pressure and temperature ranges of 10.0 -34.0MPa and 308 -338K, respectively. 500 mg of AV3RN powder was thoroughly mixed with adequate amount of glass beads; it was then packed in a solubility cell. A metallic sintered filter was also used on both sides of the cell to retain the solute in the equilibrium cell. Under operation conditions, sc-CO_2 pressure was increased to a required pressure; it was then passed through the solubility cell. About the ending of the static time, 500 µL saturated sc-CO_2 was then entered in the injection loop using the ten-port, two-status valve. By switching the injection valve, the loop pressure will be decreased in the collection vial encompassing a given amount of methanol. At the end of the procedure, a micrometer-scaled valve was applied to adjust the depressurization stage to prevent from the solvent dispersion. Finally, the valve was fully opened; the sample loop was cleaned by methanol and the resulting solution was stored in a collection vial. The final volume was 5 mL. The solubility values of AV3RN under different conditions were recorded by absorbance evaluation at λ_{max} of each sample through use of a UV–vis spectrophotometer (Cecil Aquarius CE 7200 double beam London, UK). The stock AV3RN solution (100 µg mL^{-1}) was prepared through dissolving the solid sample in methanol. A series of standard solutions was obtained by proper dilution of the stock solution. The solute concentrations in the collection vial were evaluated by calibration curves (with regression coefficients of ~0.998). UV absorption of AV3RN was quantitatively analyzed at 600 nm.
Experimental density-based correlations are one of the widely used thermodynamic approaches for modeling the solid solubility in supercritical fluids (SCFs). Empirical models rely on a linear association between the solubility logarithm and the solvent density logarithm (or the solvent density itself) near its critical regime, with the system-dependent appropriate ordinate. Although various empirical models have been developed, no comprehensive model has been introduced which could be appropriately applied for different series of solubility data.
In this work, four empirical models proposed by Chrastil [5], Bartle *et al.* [6], Garlapati-Madras [7] and Khansary *et al.* [8] were utilized for correlating the empirical solubility results (Table 1). The constants in the models were estimated by regression of experimental data. In these models "y" denotes the mole fraction of AV3RN in AV3RN / sc-CO_2 system, "ρ" and "T" represent the pure supercritical phase density (kg m^{-3}) and temperature (K), respectively. Also, "ρ_{ref}" in Bartel *et al.* model represents the reference density (700 kg m^{-3}) and "P_{ref}" indicates the reference pressure (0.1 MPa). Accuracy of mentiond models are investigated by calculation of average absolute relative deviation (AARD), R_{adj} and F-value as follows:

$$AARD\% = \frac{1}{N}\sum_{i=1}^{n}\left(\left|\frac{y_{i,cal} - y_{i,\exp}}{y_{i,\exp}}\right|\right)\times 100\% \quad (1)$$

Where "$y_{i,exp}$" and "$y_{i,calc}$" represent the empirical and computational solubility values, respectively. "N" stand for the number of data points for each set and model. As another comparison, R_{adj} is defined as follows [9]:

$$R_{adj} = \sqrt{\left|R^2 - (Q(1-R^2)/(N-Q-1))\right|} \quad \& \quad R^2 = 1 - \frac{SS_E}{SS_T} \quad (2)$$

In the above equation, the number of independent variables is shown by "Q" while R^2 represents the correlation coefficient.Also, "SS_E" and "SS_T" denote the error and total sum of squares, respectively Given that R_{adj} indicates the number of independent variables, it is applicable for comparing the models. Fitting ability of the model could be assessed by F-value:

$$F - value = \frac{SS_R/Q}{SS_E/(N-Q-1)} = \frac{MS_R}{MS_E} \quad (3)$$

In which, "SSR" stands for the regression sum of squares; "MS_R" denotes the mean square regression and "MS_E" represents the mean square residual. F-value distribution has an F statistic form possessing Q and N-Q-1 degrees of freedom [10].

Table 1: Summary of the empirical models used in this work

Model	Formula	Number of constants
Chrastil	$\ln y = a_0 + a_1 \ln(\rho) + \frac{a_2}{T} \qquad \Delta H_t = -a_2.R$	3
Bartle *et al.*	$\ln \frac{y.P}{P_{ref}} = a_0 + a_1(\rho - \rho_{ref}) + \frac{a_2}{T} \qquad \Delta H_{vap} = -a_2.R$	3
Garlapati-Madras	$\ln y = a_0 + (a_1 + a_2\rho)\ln\rho + \frac{a_3}{T} + a_4 \ln(\rho T)$	5
Khansary *et al.*	$\ln y = \frac{a_0}{T} + a_1 P + \frac{a_2 P^2}{T} + (a_3 + a_4 P)\ln(\rho)$	5

Results and discussion

Table 2 lists the sc-CO_2 densities (from NIST web-book (http://webbook.nist.gov/chemistry)) and solubility data of AV3RN at different pressures and temperatures in terms of solubility (S) and AV3RN equilibrium mole fraction (y_2) in which the reported data points are the average (standard error of the mean (SEM)) of three replicates with relative standard deviations below 5%.

Solubility of AV3RN vs. pressure and sc-CO_2 density at constant temperatures is plotted in Fig.(1a) and Fig.(1b), respectively. An increment in solubility with increase of pressure at constant temperature is evident in Fig.(1a) which was intensified at higher temperatures and could be attributed to a decline in distance between CO_2 molecules at higher pressures and increase of sc-CO_2 density that could enhance the AV3RN-CO_2 interactions; therefore improving the solvation power of sc-CO_2 [11]. The two competing parameters (opposite temperature dependence of solute vapor pressure and sc-CO_2 density) made the temperature impact on solubility more complicated. It was demonstrated by the presence of crossover points, in which the temperature and pressure approached to the critical fluid state. Crossover pressure region lied in 13 -17 MPa range in Fig. 1a. At higher pressures, over the crossover

region, temperature enhancement led to the improved solubility values ($y_{338} > y_{328} > y_{318} > y_{308}$) which may be attributed to the increased AV3RN vapor pressure. At lower pressures, however, the temperature and solubility variations opposed each other due to a reduction in the sc-CO_2 density at high temperatures which resulted in decline of the solubility [12,13].

Table 2: Solubility data of AV3RN in sc-CO_2 at different temperatures (T) and pressures (P)

T (K)	P (bar)	ρ (kg m^{-3})	y × 10^5 ± standard *deviation* [c]	S × 10^3 (kg m^{-3}) [d]
308	100	714.84	0.07 ± 0.014	7.08
	120	768.42	0.125 ±0.004	13.59
	160	828.10	0.178 ± 0.002	20.86
	200	866.48	0.22 ± 0.009	26.97
	240	895.54	0.261± 0.005	33.07
	300	929.68	0.344 ±0.01	45.25
	340	948.48	0.391± 0.004	52.47
318	100	502.57	0.062 ± 0.003	4.41
	120	659.73	0.111± 0.002	10.36
	160	761.07	0.139 ± 0.0042	14.97
	200	813.52	0.27 ± 0.003	31.08
	240	850.1	0.331± 0.013	39.81
	300	890.92	0.399 ± 0.008	50.30
	340	912.69	0.443 ± 0.014	57.21
328	100	326.4	0.055 ± 0.003	2.54
	120	506.85	0.101± 0.004	7.24
	160	682.39	0.172 ± 0.0034	16.61
	200	755.52	0.319 ± 0.01	34.10
	240	801.92	0.367 ± 0.004	41.64
	300	850.83	0.471 ± 0.023	56.70
	340	876.03	0.519 ± 0.01	64.33
338	100	266.47	0.047 ± 0.0014	1.77
	120	384.17	0.099 ± 0.004	5.38
	160	593.75	0.157 ± 0.006	13.19
	200	692.68	0.371 ± 0.004	36.36
	240	751.17	0.427 ± 0.021	45.38
	300	809.58	0.5 ± 0.015	57.28
	340	838.65	0.546 ± 0.011	64.79

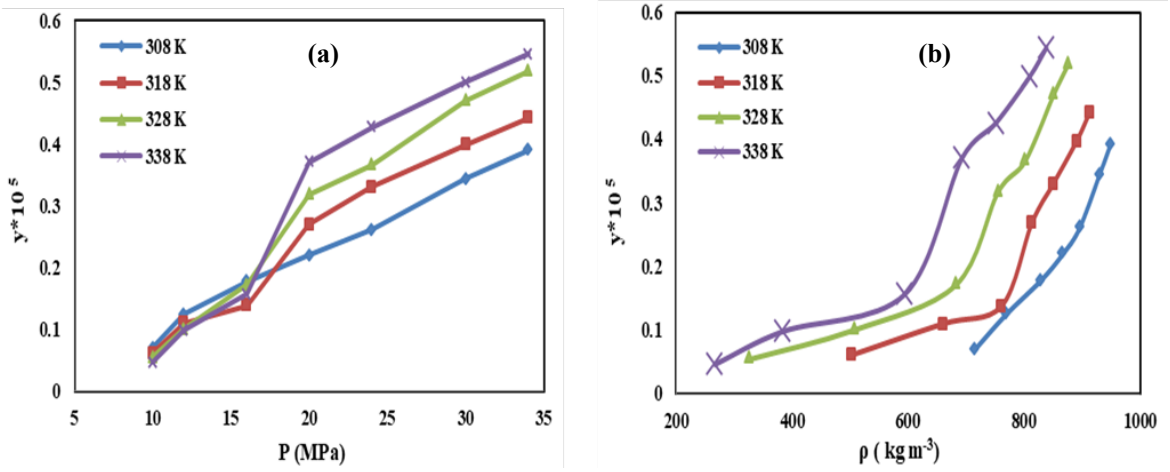

Fig. (1): AV3RN solubility in sc-CO_2 at various temperatures vs. (a) pressure and (b) sc-CO_2 density.

As shown in Fig.1, AV3RN solubility values is varied from 4.7 × 10^{-7} to 5.5 × 10^{-6} mole fraction, depending on the temperature and pressure. The highest and lowest AV3RN solubilities were observed at single temperature (338 K) but various pressure values: 340 bar and 100 bar, respectively. As previously mentioned, four well-known empirical models were applied to correlate the solubilities of AV3RN in sc-CO_2. Adjustable parameters of these models were optimized by MATLAB optimization function under different pressures. The adjustable parameters of each empirical model along with their AARD, R_{adj} and F-values are listed in Table 3. Moreover, correlated findings from these density-based models and experimental results are illustrated in Figs. (2a-f). As shown in Table 3, Bartle *et al*. model (AARD of 28.6%, R_{adj} of 0.94) showed the highest deviation from experimental data. As expected, models with higher adjusted variables exhibited higher accuracies. So, the Khansary *et al*. model (AARD of 11.3%, R_{adj} of 0.98) and Garlapati-Madras model (AARD of 13%, R_{adj} of 0.98) possessed the lowest absolute deviation. Consequently, these models are capable of better correlating, validating and predicting the empirically measured AV3RN solubility values at proper temperatures and pressures. These results can also be confirmed by the correlation results presented in Fig 2.

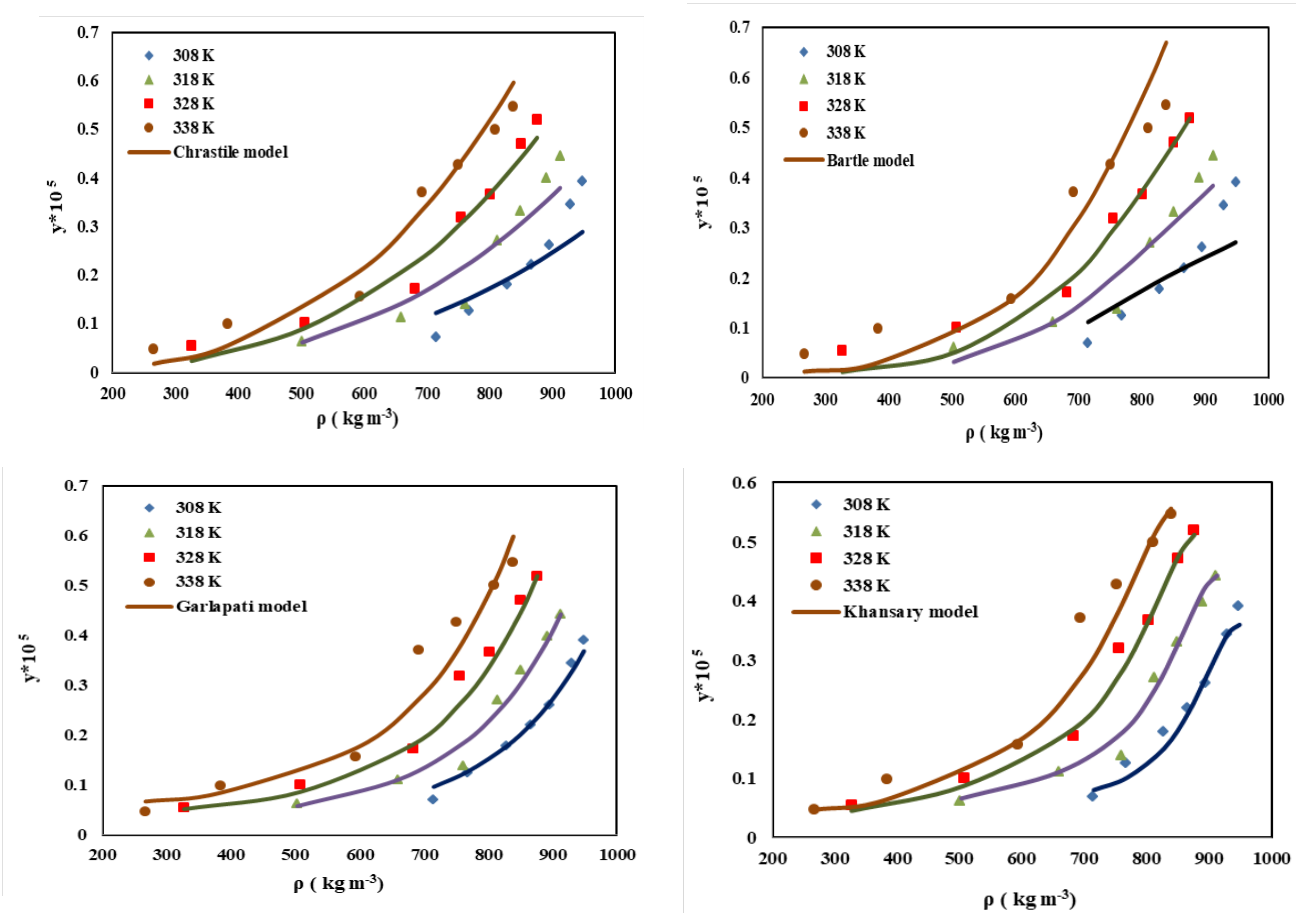

Fig. (2): Comparison of experimental (points) and calculated (line) solubility of AV3RN in the binary AV3RN/sc-CO_2 system; a) Chrastil's models, b) Bartle *et al*., c) Garlapati *et al*., d) Khansary *et al*. models at various conditions.

As shown in Table 1, some of the AV3RN properties such as its total reaction heat (ΔH_t) and vaporization enthalpy ($\Delta H_{vap.}$) can be obtained by utilization of "a_2" adjustable parameters of Chrastil's model and Bartle model, respectively. In Chrastil's model, $a_2 = -\Delta H_t/R$ in which R stands for the gas constant and ΔH_t shows the summation of solute vaporization ($\Delta H_{vap.}$) and solvation ($\Delta H_{sol.}$) enthalpies, based on Hess's rule. Therefore, it can be concluded that "a_2" is a function of total reaction heat (ΔH_t). Also in Bartle model, the solute vaporization heat ($\Delta H_{vap.}$) can be estimated by direct use of "a_2" parameter ($a_2 = -\Delta H_{vap}/R$). Also, difference of calculated ΔH_t and $\Delta H_{vap.}$ represents the solvation heat ($\Delta H_{sol.}$). Accordingly, total reaction heat (ΔH_t), solute vaporization enthalpy ($\Delta H_{vap.}$) and solvation heat ($\Delta H_{sol.}$) are calculated as 322.5 J mol^{-1}, 543.73 J mol^{-1} and -221.23 J mol^{-1} , respectively.Clearly, AV3RN evaporation is an endothermic process while its solvation is an exothermic process.

Table 3: Correlation results of AV3RN solubility in sc-CO_2 through various empirical models

Model	Adjustable parameters					AARD/ %	R_{adj}	F-value
	a_0	a_1	a_2	a_3	a_4			
Chrastil	-0.22	3.04	-38.8			25.3	0.96	100.46
Bartle *et al.*	12.145	9.03	-65.4			28.6	0.94	66.03
Garlapati - Madras	-5.62	-0.074	5.76	-3697.6	0.95	13	0.98	199.1
Khansary *et al.*	-4688.8	0.022	-0.011	-1.61	0.036	11.3	0.98	244.2

Conclusions

The current study addressed the experimental solubility of Anthraquinone Violet 3RN (AV3RN) in supercritical carbon dioxide (sc-CO_2). Various temperatures 308-338K and pressures 10-34MPa were considered. The solubilities were reported as 4.7×10^{-7} to 5.5×10^{-6}. Additionally, the experimental solubility data were correlated to several density-based models. This research indicated that the Khansary *et al*. model and Garlapati-Madras model in binary AV3RN/sc-CO_2 system managed to exhibit a proper agreement with the empirical solubilities. Regarding the capability of these models in correlating the experimental AV3RN solubilities under proper temperature and pressure values, they can lead to superior results.

References

[1] Y. Caro, L. Anamale, M. Fouillaud, P. Laurent, T. Petit, L. Dufosse, Natural hydroxyanthraquinoid pigments as potent food grade colorants: an overview, Nat. Prod. Bioprospect. 2 (2012) 174-193.

[2] J. Sánchez-Martín, J. Beltrán-Heredia, C. Solera-Hernández, Surface water and wastewater treatment using a new tannin-based coagulant. Pilot plant trials, J. Environ. Manage. 91 (2010) 2051-2058.

[3] L. Miah, N. Ferdous, D. Azad, Textiles Material Dyeing with Supercritical Carbon Dioxide (CO_2) without using Water, Chem. Mater. Res.3 (2013) 38-40.

[4] J. Beltrán-Heredia, J. Sánchez-Martín, A .Delgado-Regalado, C. Jurado-Bustos, Removal of Alizarin Violet 3R (anthraquinonic dye) from aqueous solutions by natural coagulants, J. Hazard. Mater. 170 (2009) 43-50.

[5] J. Chrastil, Solubility of solids and liquids in supercritical gases, J. Phys. Chem. 86 (1982) 3016-3021

[6] K.D. Bartle, A.A. Clifford, S.A. Jafar, G.F. Shilstone, Solubilities of Solids and Liquids of Low Volatility in Supercritical Carbon Dioxide, J. Phys. Chem. Ref. Data 20 (1991) 713-756.

[7] C. Garlapati, G. Madras, New empirical expressions to correlate solubilities of solids in supercritical carbon dioxide, Thermochim. Acta 500 (2010) 123-127.

[8] M. Asgarpour Khansary, F. Amiri, A. Hosseini, A. Hallaji Sani, H. Shahbeig, Representing solute solubility in supercritical carbon dioxide: A novel empirical model, Chem. Eng. Res. Des. 93 (2015) 355-365.

[9] T. Abou Elmaaty, E. Abd El-Aziz, Supercritical carbon dioxide as a green media in textile dyeing: A review, Text. Res. J. 88 (2018) 1184-1212.

[10] S.-H. Cheng, F.-C. Yang, Y.-H. Yang, C.-C. Hu, W.-T. Chang, Measurements and modeling of the solubility of ergosterol in supercritical carbon dioxide, J. Taiwan Inst. Chem. Eng. 44 (2013) 19-26.

[11] K. Tamura, R.S. Alwi, Solubility of anthraquinone derivatives in supercritical carbon dioxide, Dyes Pigm. 113 (2015) 351-356

[12] R.S. Alwi, T. Tanaka, K. Tamura, Measurement and correlation of solubility of anthraquinone dyestuffs in supercritical carbon dioxide, J. Chem. Thermodyn. 74 (2014) 119-125.

[13] Z.B. Loubna Nasri, Solubility of Solids in Supercritical Fluids: The Mendez-Santiago Teja Model Revisited, Adv. Chem. Eng. Sci. 5 (2015) 413-423.